



## Design of planar four-bar linkage with $n$ specified positions for a flapping wing robot



Jing-Shan Zhao\*, Zheng-Fang Yan, Li Ye

State Key Laboratory of Tribology, Department of Mechanical Engineering, Tsinghua University, Beijing 100084, PR China

### ARTICLE INFO

#### Article history:

Received 26 January 2014

Received in revised form 2 July 2014

Accepted 3 July 2014

Available online xxxx

#### Keywords:

Flapping wing robot

Multi-position design

Planar four-bar linkage

Burmester's theory

### ABSTRACT

This paper focuses on the design of a flapping wing robot and proposes a unified design formula for planar four-bar linkages with arbitrary  $n$  prescribed positions. The absolute coordinates of a circle point corresponding to every prescribed position are expressed by those of the first one through matrix transformation. Because the distance between any circle point and center point is always equal to the length of the side link jointed with the fixed base, a set of quadratic equations for the distance constraints are obtained. Expanding and rearranging these equations presents a linear system for the coordinates of center point. The condition for existing solution of these equations requires that the rank of the augmented rectangle coefficient matrix,  $\mathbf{C}$ , should always be less than 3 as there are only two unknown coordinates for the center point. The rectangle augmented coefficient matrix  $\mathbf{C}$  is  $(n - 1) \times 3$ , and therefore it can be transformed to a  $3 \times 3$  square matrix,  $\mathbf{M}$ , by left multiplying the transpose of  $\mathbf{C}$ . This provides a unified expression for the design of a planar four-bar linkage with arbitrary  $n$  positions for a flapping wing.

© 2014 Elsevier Ltd. All rights reserved.

## 1. Introduction

Bionic robotics research has been focused on the development of flapping wing machines from the natural flight mechanism of insect or bird, which are foreseen to have better performance. Examples can be found, such as the dragonflies [1], hawkmoths [2], doves [3], bats [4], and so on [5]. In most cases, the wing of a bird usually executes a periodic flapping motion. So it is the primary target to synthesize such an oscillating process with a simple mechanism when one aims at designing an unmanned aerial vehicle to mimic the bird's flight. Linkages have been applied to human's life ever since the ancient time [6]. And the planar four-bar linkage as a typical and simple mechanism can be used to simulate the flapping motion of a bird. For the design of a planar four-bar linkage, the Burmester problem as a classical issue has been extensively discussed in the previous literature. To uncover the physical relationship between linkage and the specified positions [7], the planar Burmester problem has been investigated by analytical methods and generalized to the spherical and spatial four-bar linkages [8–12].

The Burmester problem was initially proposed by Ludwig Burmester to analyze the geometric constraints of the linkage directly from the desired movement for a floating link [13]. It is the motion design objective for a planar four-bar linkage to calculate the mechanism parameters required to achieve a set of specified coupler poses which includes the positions and orientations of a link [14]. It is the design target of a planar four-bar linkage to find a point from the floating link that lies on a circle when viewed in each of these specified coupler poses. That is to say, the revolute joints of the side links, which are also called *center points*, must be located within a certain area of the fixed frame [15]. This mechanism design target is particularly useful when the coupler must achieve a specific displacement sequence for effective operation. The point on the floating link is called *circle point* when its circular trajectory center

\* Corresponding author. Fax: +86 10 62788308.

E-mail address: [jingshanzhao@mail.tsinghua.edu.cn](mailto:jingshanzhao@mail.tsinghua.edu.cn) (J.-S. Zhao).

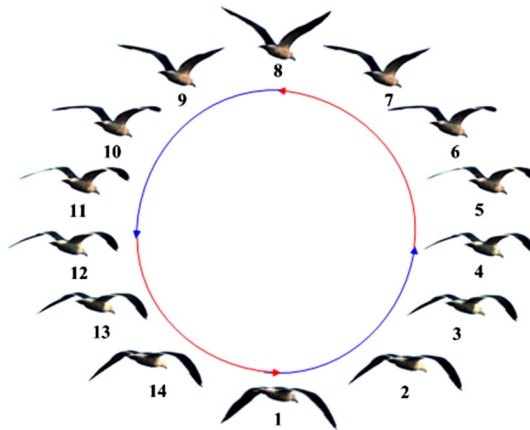


**Fig. 1.** Periodic motion in flying.

is superimposed with the *center point* [16]. Burmester's *circle point* and *center point* curves are used to determine the dimensions of a planar four-bar linkage [17–21]. This formulation of the mathematical synthesis of a four-bar linkage and the solution is generally called Burmester's Theory [22–24]. In Burmester's classical textbook, the circle point and center point and some biographical data about Burmester are thoroughly introduced [25]. As certain fundamental ideas of mechanism return with some regularity to the methodology of machine design [26] historical surveys [27–29] trace the early events relating to machine inventions and applications of linkages that were originally expounded by Reuleaux. Analytical studies of the properties of coupler curves commenced in 1875 [27], when Samuel Roberts published the first account of the algebraic properties of the planar four-bar curve. Planar synthesis for orderly progression through four specified positions can be solved with Burmester's theory [30,31]. Koetsier commented on the Burmester's theory [16] and its importance to the development of planar linkage synthesis [25].

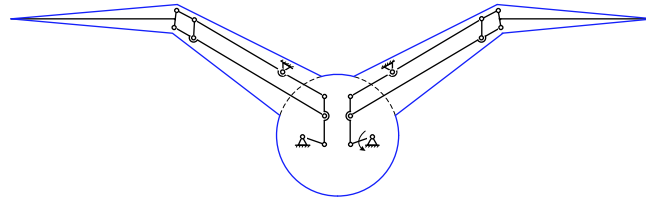
However, there are still three problems that have to be considered in the synthesis: branch, order and crank problem [30]. Different methods have been proposed to solve the problem [17,18,32]. In addition, the crank center must be located within certain areas of a fixed plane. The result shows that these areas can be determined in advance. Simple extensions of the analysis offer a detailed picture of the movements of both driving crank and followers. Complex number method [33] was applied to the dimensional synthesis of planar triads for six exact positions and motion generation. For four specified task positions for the design of planar four-bar linkage, Burmester curve equations can be represented by displacement matrix method [34,35]. The synthesis of a planar four-bar linkage was discussed to generate a coupler-line envelope, tangent to three, four and five prescribed link positions, and to coordinate the coupler-line movements with two, three and four input-link positions [36]. However, the loci of the center-point and of the circle-point of the driving link in the four-position case are eight concurrent straight lines, and the loci in the five-position case might be 64 points. So it is a great challenge for the engineers to directly use them in applications. Therefore, this paper focuses on the planar four-bar linkage and investigates the multiposition design for a flapping wing.

## 2. Unified formula of planar four-bar linkages with $n$ specified position

The wing of a bird usually executes a periodic motion in flying which can be roughly shown by Fig. 1. The flying direction of the bird in Fig. 1 is from rear left to front right. Position 1 through position 8 anticlockwise illustrates the flight of upstroke and position 8 through position 14 shows the flight of downstroke of the bird. Position 1 represents the start of upstroke or the end of downstroke while position 8 illustrates the start of downstroke or the end of up-stroke. Trajectory generation for the flapping wing is the focus of design which has been a subject of extensive research in formation flying spacecraft [37]. These problems are difficult to solve in general. To effectively simulate the flapping process of a bird, 8 key poses during the upstroke of a seagull as Fig. 2 illustrates are



**Fig. 2.** Eight crucial positions during the upstroke and downstroke.

**Fig. 3.** A planar linkage.

particularly selected. These eight positions, as the right case of Fig. 2 indicates, are the crucial positions that the four-bar linkage should successively achieve in the periodic flapping flight.

Firstly, the initial mechanism to achieve the fly of a seagull is designed. The major part of the mechanism to imitate the wing's flapping is a planar linkage shown in Fig. 3. Because of the symmetrical structure of the wings, it is enough to analyze the right part shown in Fig. 4. Since eight positions of the linkage for the flapping wing of a seagull have been proscribed, the eight sets of positions of the rigid link  $PQH$  in Fig. 4 are known. So the design has now been changed to the synthesis of a planar four-bar linkage with these 8 positions. In the next section, the general requirements for multiposition design of a planar four-bar linkage will be first discussed in general.

## 2.1. General requirements for multiposition design of a planar four-bar linkage

Suppose that the link of a planar four-bar linkage shown in Fig. 5 is required to successively pass through a number of specified positions,  $P_1Q_1, P_2Q_2, \dots, P_nQ_n (n \geq 3)$ . It is the target of position synthesis to find the pivots on the fixed base and the floating link as well.

Fig. 6(a) illustrates the case that links  $P_1Q_1$  is in the first position. In the absolute coordinate system, the position is represented by the absolute coordinates of point  $P_1$  and the rotational angle,  $\theta_1$ , about the z-axis which is perpendicular to the  $xoy$ -plane in the absolute coordinate system and is therefore not marked in Fig. 6. Assume that the pivots on the link corresponding to the first position are denoted by  $B_1$  and  $C_1$ . When the  $i$ th ( $i \leq n$ ) position,  $P_iQ_i$  shown in Fig. 6(b), is specified, the transformation from the first coordinate system,  $x_1P_1y_1$ , to the  $i$ th one,  $x_iP_iy_i$ , can be uniquely determined:

$$\mathbf{r}_{B_i} = \mathbf{r}_{P_1} + \mathbf{r}_{P_1P_i} + \mathbf{R}(\theta_{1i})\mathbf{r}_{P_1B_1} \quad (2.1)$$

where  $\mathbf{r}_{B_i}$  denotes the absolute vector of joint  $B_i$ ,  $\mathbf{r}_{P_1}$  denotes the absolute vector of joint  $P_1$ ,  $\mathbf{r}_{P_1P_i}$  denotes the absolute vector of  $\overrightarrow{P_1P_i}$ ,  $\mathbf{r}_{P_1B_1}$  denotes the absolute vector of  $\overrightarrow{P_1B_1}$ , and

$$\mathbf{R}(\theta_{1i}) = \begin{bmatrix} \cos\theta_{1i} & -\sin\theta_{1i} \\ \sin\theta_{1i} & \cos\theta_{1i} \end{bmatrix} \quad (2.2)$$

where  $\theta_{1i} = \theta_i - \theta_1$ .

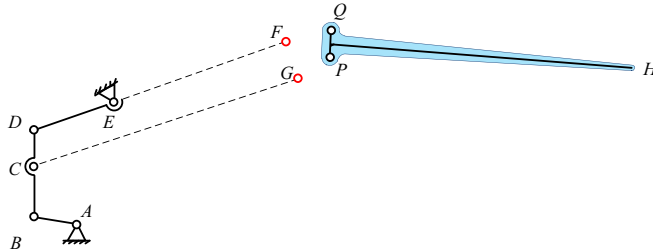
Because

$$\mathbf{r}_{P_i} = \mathbf{r}_{P_1} + \mathbf{r}_{P_1P_i} \quad (2.3)$$

and  $\mathbf{r}_{P_i}$  is prescribed, Eq. (2.1) can also be simplified as

$$\mathbf{r}_{B_i} = \mathbf{r}_{P_i} + \mathbf{R}(\theta_{1i})\mathbf{r}_{P_1B_1}. \quad (2.4)$$

For the joints  $B_1, B_2, \dots$ , and  $B_i$  are all circle points, they must locate on a circle whose center is the fixed pivot on the base and which is denoted by  $A$  in Fig. 7.

**Fig. 4.** Basic part to generate the flapping motion.

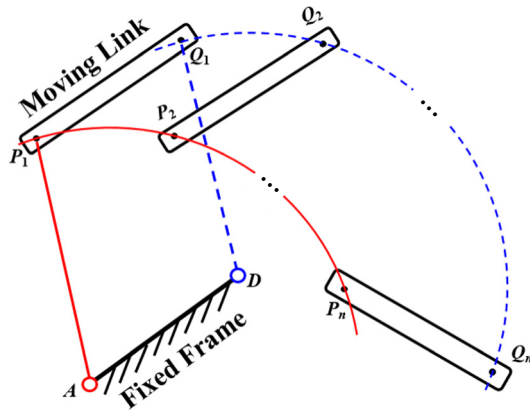


**Fig. 5.** General multiposition synthesis of planar four-bar linkage.

Immediately, the following equations are obtained

$$\|\mathbf{r}_{AB_i}\|^2 = \|\mathbf{r}_{AB_1}\|^2 \quad (i = 2, 3, \dots, n) \quad (2.5)$$

where  $\mathbf{r}_{AB_i} = \mathbf{r}_{B_i} - \mathbf{r}_A = \mathbf{r}_{P_i} + \mathbf{R}(\theta_{1i})\mathbf{r}_{P_1B_1} - \mathbf{r}_A$ ,  $\mathbf{r}_{AB_1} = \mathbf{r}_{B_1} - \mathbf{r}_A$ ,  $\|\cdot\|$  represents the Euclidean norm of vector “·”,  $\mathbf{r}_{AB_i}$  denotes the absolute vector of  $\overrightarrow{AB_i}$ ,  $\mathbf{r}_{AB_1}$  represents the absolute vector of  $\overrightarrow{AB_1}$ ,  $\mathbf{r}_A$  denotes the absolute vector of joint A.

Expanding Eq. (2.5) presents

$$c_{i1}x_A + c_{i2}y_A + c_{i3} = 0 \quad (2.6)$$

where  $i = 2, 3, \dots, n$ ,  $x_A$  and  $y_A$  denote the absolute coordinates of center point A, and

$$\begin{cases} c_{i1} = 2[x_{B_1}(1 - \cos\theta_{1i}) + y_{B_1} \sin\theta_{1i} + x_{P_1} \cos\theta_{1i} - y_{P_1} \sin\theta_{1i} - x_{P_i}] \\ c_{i2} = 2[y_{B_1}(1 - \cos\theta_{1i}) - x_{B_1} \sin\theta_{1i} + y_{P_1} \cos\theta_{1i} + x_{P_1} \sin\theta_{1i} - y_{P_i}] \\ c_{i3} = 2(-x_{P_i}y_{B_1} - y_{P_i}x_{P_1} + x_{P_i}y_{P_1} + y_{P_i}x_{B_1}) \sin\theta_{1i} \\ \quad + 2(x_{P_i}x_{B_1} - x_{P_i}x_{P_1} - y_{P_i}y_{P_1} + y_{P_i}y_{B_1}) \cos\theta_{1i} \\ \quad - 2y_{B_1}y_{P_1} - 2x_{B_1}x_{P_1} + y_{P_i}^2 + x_{P_i}^2 + y_{P_1}^2 + x_{P_1}^2 \end{cases} \quad (2.7)$$

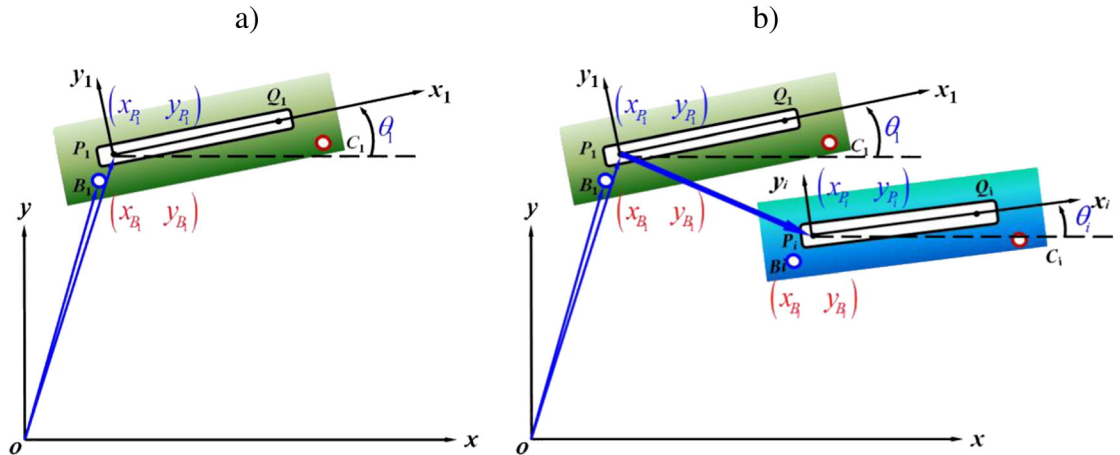


**Fig. 6.** Transformation between two positions.

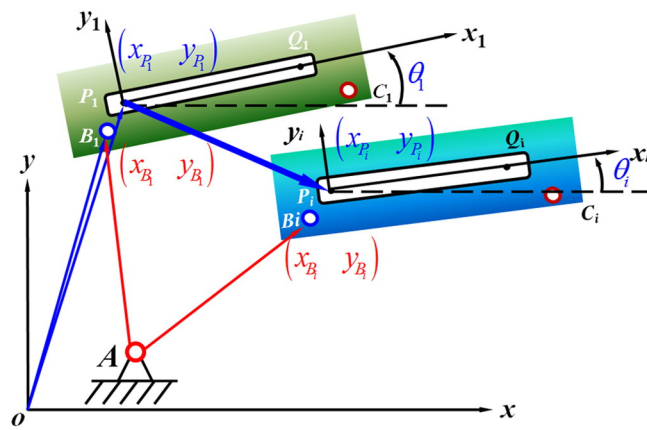


**Fig. 7.** Circle point and center point.

When 3 specified positions of the link are known, the following equation set should hold:

$$\begin{cases} c_{21}x_A + c_{22}y_A + c_{23} = 0 \\ c_{31}x_A + c_{32}y_A + c_{33} = 0 \end{cases} \quad (2.8)$$

Solving Eq. (2.8), one obtains that

$$\begin{cases} x_A = -\frac{\begin{vmatrix} c_{23} & c_{22} \\ c_{33} & c_{32} \end{vmatrix}}{\begin{vmatrix} c_{21} & c_{22} \\ c_{31} & c_{32} \end{vmatrix}} \\ y_A = -\frac{\begin{vmatrix} c_{21} & c_{23} \\ c_{31} & c_{33} \end{vmatrix}}{\begin{vmatrix} c_{21} & c_{22} \\ c_{31} & c_{32} \end{vmatrix}} \end{cases} \quad (2.9)$$

Eq. (2.7) indicates that the coefficients of the linear equation set in Eq. (2.8) are the function of the coordinates of joint  $B_1$ , therefore there is one solution expressed by Eq. (2.9) when joint  $B_1$  is directly prescribed as point  $P_1$ . There will be other solutions when joint  $B_1$  is changed to another one within the plane determined by link  $P_1Q_1$ . Therefore, there are infinite solutions for the 3-position design of a planar four-bar linkage. When 4 specified positions of the floating link are provided, the following equation set holds:

$$\begin{cases} c_{21}x_A + c_{22}y_A + c_{23} = 0 \\ c_{31}x_A + c_{32}y_A + c_{33} = 0 \\ c_{41}x_A + c_{42}y_A + c_{43} = 0 \end{cases} \quad (2.10)$$

Equation set in Eq. (2.10) only has 2 unknowns, namely  $x_A$  and  $y_A$ , but there are 3 equations. Therefore, only 2 independent equations in equation set (2.10) are necessary to determine the coordinates of joint A. In other words, the sufficient and necessary condition that Eq. (2.10) has a solution is

$$R(\mathbf{C}_{3 \times 3}) \leq 2 \quad (2.11)$$

where  $R(\cdot)$  denotes the rank of matrix “ $\cdot$ ” and  $\mathbf{C}_{3 \times 3} = \begin{bmatrix} c_{21} & c_{22} & c_{23} \\ c_{31} & c_{32} & c_{33} \\ c_{41} & c_{42} & c_{43} \end{bmatrix}$ . Therefore the conditions that there are solutions for the coordinates of center point A can be alternatively expressed as

$$|\mathbf{C}_{3 \times 3}| = 0 \quad (2.12)$$

**Table 1**

Four specified positions for the floating link.

Items	1st position	2nd position	3rd position	4th position
x-Coordinate (mm)	0	4	1	3
y-Coordinate (mm)	-5	3	6	5
Pose angle (°)	90	45	-60	30

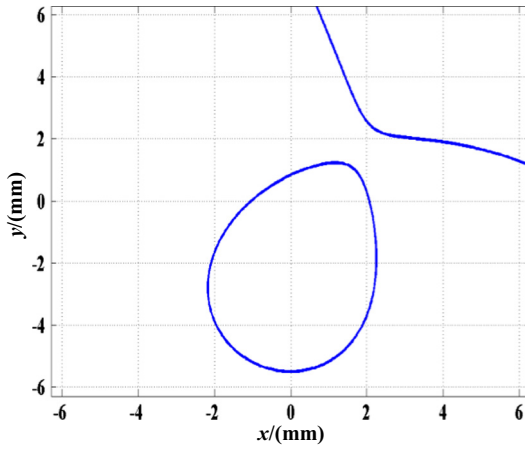


**Fig. 8.** Circle point curve of 4-position design.

where  $|\cdot|$  represents the determinant of matrix “ $\cdot$ ”. Eq. (2.7) indicates that every element of the determinant in Eq. (2.12) is a linear function of the coordinates of circle point  $B_1$ . Eq. (2.12) represents a 3rd order curve of the coordinates of point  $B_1$ .

When 5 specified positions of the link are known, the following equation set should hold:

$$\begin{cases} c_{21}x_A + c_{22}y_A + c_{23} = 0 \\ c_{31}x_A + c_{32}y_A + c_{33} = 0 \\ c_{41}x_A + c_{42}y_A + c_{43} = 0 \\ c_{51}x_A + c_{52}y_A + c_{53} = 0 \end{cases} \quad (2.13)$$

Equation set in Eq. (2.13) also has 2 unknowns,  $x_A$  and  $y_A$ , but there are 4 equations. Only 2 independent equations in equation set (2.13) are needed to decide the coordinates of joint  $A$ . In other words, the sufficient and necessary conditions that Eq. (2.13) has a solution are

$$R(\mathbf{C}_{4 \times 3}) < 3 \quad (2.14)$$

where  $\mathbf{C}_{4 \times 3} = \begin{bmatrix} c_{21} & c_{22} & c_{23} \\ c_{31} & c_{32} & c_{33} \\ c_{41} & c_{42} & c_{43} \\ c_{51} & c_{52} & c_{53} \end{bmatrix}$ . The number of 3-order determinants is a combination of selecting 3 rows from the 4 rows of matrix  $\mathbf{C}_{4 \times 3}$  which can be denoted by  $\binom{4}{3}$  where  $\binom{m}{n}$  indicates the combination of  $n$  from  $m$ . So there should be  $\binom{4}{3} = 4$  equations of 3-order determinants if Eq. (2.14) is replaced by the zero-determinant expressions. Namely,

$$\left\{ \begin{array}{l} \left| \begin{array}{ccc} c_{21} & c_{22} & c_{23} \\ c_{31} & c_{32} & c_{33} \\ c_{41} & c_{42} & c_{43} \end{array} \right| = 0 \\ \left| \begin{array}{ccc} c_{31} & c_{32} & c_{33} \\ c_{41} & c_{42} & c_{43} \\ c_{51} & c_{52} & c_{53} \end{array} \right| = 0 \\ \left| \begin{array}{ccc} c_{41} & c_{42} & c_{43} \\ c_{51} & c_{52} & c_{53} \\ c_{21} & c_{22} & c_{23} \end{array} \right| = 0 \\ \left| \begin{array}{ccc} c_{51} & c_{52} & c_{53} \\ c_{21} & c_{22} & c_{23} \\ c_{31} & c_{32} & c_{33} \end{array} \right| = 0 \end{array} \right. \quad (2.15)$$

**Table 2**

Five specified positions for the floating link.

Items	1st position	2nd position	3rd position	4th position	5th position
$x$ -coordinate (mm)	10	−6	−13	−17	6
$y$ -coordinate (mm)	−5	−22	−11	10	5
Pose angle ( $^{\circ}$ )	0	−26	−40	−48	−15

**Table 3**

Four solutions for the specified 5-position problem.

$x_{B_1}$ (mm)	$y_{B_1}$ (mm)	$x_A$ (mm)	$y_A$ (mm)
-30.568446	20.960137	191.467702	-64.838556
26.545161	32.179730	-44.146967	-17.273592
-0.818763	64.804165	-13.399540	-60.318106
38.477471	3.216875	-25.700624	9.351623

The circle point  $B_1$  must be the intersection of these four 3-order curves represented by Eq. (2.15). Similarly, when  $n$  specified positions of the link are given, the following equation set should hold if there is one solution at least:

$$\begin{cases} c_{21}x_A + c_{22}y_A + c_{23} = 0 \\ c_{31}x_A + c_{32}y_A + c_{33} = 0 \\ \vdots \\ c_{n1}x_A + c_{n2}y_A + c_{n3} = 0 \end{cases} \quad (2.16)$$

where  $n = 3, 4, \dots$ .

Equation set in Eq. (2.16) also has 2 variables,  $x_A$  and  $y_A$ , but there are  $n - 1$  constraint equations. Therefore, only 2 in equation set (2.16) are required to determine the coordinates of joint A. Hence the sufficient and necessary conditions that equation set (2.16) has a solution could be expressed as

$$R(\mathbf{C}_{(n-1) \times 3}) < 3 \quad (2.17)$$

where

$$\mathbf{C}_{(n-1) \times 3} = \begin{bmatrix} c_{21} & c_{22} & c_{23} \\ c_{31} & c_{32} & c_{33} \\ \vdots & \vdots & \vdots \\ c_{(n-1)1} & c_{(n-1)2} & c_{(n-1)3} \end{bmatrix}. \quad (2.18)$$

There should be  $\binom{n-1}{3} = \frac{(n-1)(n-2)(n-3)}{6}$  equations of 3-order determinants when Eq. (2.17) is equivalently represented as that the determinants of all  $3 \times 3$ -matrices are zeros simultaneously. It is a tricky job to search the intersections of so many 3-order curves.

## 2.2. Formula for the design of a planar four-bar linkage

When  $n$  specified positions of the link are known, the condition that there is one solution at least is that the rank of the augmented coefficient matrix will always be less than 3. The solution might be expressed as that the determinant of the square matrix is zero if a  $3 \times 3$ -matrix could be conceived with the augmented coefficient matrix in Eq. (2.18). Suppose

$$\mathbf{M} = \mathbf{C}_{(n-1) \times 3}^T \mathbf{C}_{(n-1) \times 3}. \quad (2.19)$$

Therefore,  $\mathbf{M}$  represented in Eq. (2.19) is a  $3 \times 3$ -matrix, and the circle points satisfying the  $n$ -position requirements must satisfy that

$$|(\mathbf{M})_{3 \times 3}| = 0 \quad (2.20)$$

**Table 4**

6 positions for a planar four-bar linkage.

Positions	$x_p$ -Coordinate (mm)	$y_p$ -Coordinate (mm)	$x_Q$ -Coordinate (mm)	$y_Q$ -Coordinate (mm)
1	1.046800	1.382700	2.577900	1.777300
2	1.127700	1.812200	2.708300	1.855700
3	0.684600	1.987400	2.264400	1.921500
4	0.119700	1.786300	1.700700	1.764300
5	-0.256500	1.325300	1.315600	1.494400
6	-0.316000	0.867500	1.189100	1.352100

**Table 5**

Solutions for the centre point and circle points for the 6-position problem prescribed in Table 4.

Circle point $B_1$ (mm)	Circle point $C_1$ (mm)	Center point $A$ (mm)	Center point $D$ (mm)
(0.749678, -0.000165)	(3.017368, 1.466613)	(-0.000396, -0.000156)	(2.700123, -0.001168)

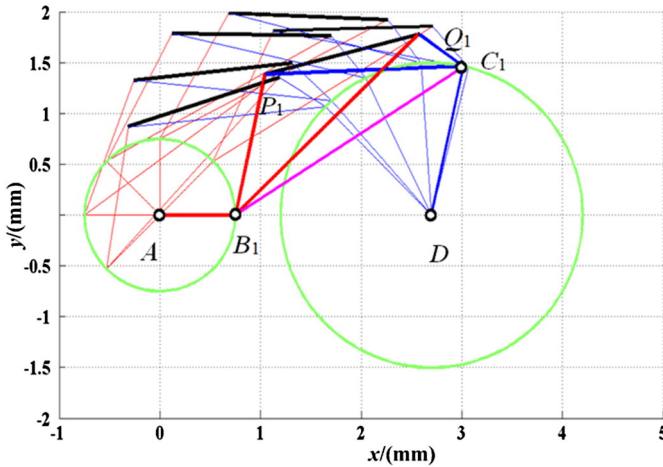


**Fig. 9.** A mechanism exactly satisfying 6 different positions.

**Proof.** For any  $n \times m$ -matrix,  $\mathbf{C}_{n \times m}$ , where  $n \geq m \geq 2$ , there is always  $R(\mathbf{C}_{n \times m}^T \mathbf{C}_{n \times m}) = R(\mathbf{C}_{n \times m})$  where  $R(\cdot)$  denotes the rank of matrix “ $\cdot$ ”. Because  $R(\mathbf{C}_{n \times m}) < m$ , the following equation must hold

$$|\mathbf{M}_{m \times m}| = 0.$$

Therefore, Eq. (2.20) is obtained by letting  $m = 3$ .

**End of proof.**

Eq. (2.20) provides a unified formula for the circle point of planar four-bar linkages with  $n$  specified positions.

However, Eq. (2.19) indicates that each element of matrix  $\mathbf{M}$  is a quadratic function of  $x_{B_1}$  and  $y_{B_1}$ , and  $\mathbf{M}$  is a positive semi-definite symmetrical matrix. So the determinant of  $\mathbf{M}$  denoted by Eq. (2.20) is greater than or equal to zero. Suppose that

$$f(x_{B_1}, y_{B_1}) = |\mathbf{M}| \quad (2.21)$$

because  $\mathbf{M}$  is a positive semi-definite symmetrical matrix,  $f(x_{B_1}, y_{B_1}) \geq 0$ . The exact solutions can be obtained when  $f(x_{B_1}, y_{B_1}) = 0$ . Otherwise, the optimum solutions for  $x_{B_1}$  and  $y_{B_1}$  of the above problem must occur when  $f(x_{B_1}, y_{B_1})$  has the minimum value. Let

$$\begin{cases} \frac{\partial f(x_{B_1}, y_{B_1})}{\partial x_{B_1}} = 0 \\ \frac{\partial f(x_{B_1}, y_{B_1})}{\partial y_{B_1}} = 0 \end{cases} \quad (2.22)$$

where  $\frac{\partial f(x_{B_1}, y_{B_1})}{\partial x_{B_1}}$  indicates the partial derivative of  $f(x_{B_1}, y_{B_1})$  with respect to  $x_{B_1}$  and  $\frac{\partial f(x_{B_1}, y_{B_1})}{\partial y_{B_1}}$  denotes the partial derivative of  $f(x_{B_1}, y_{B_1})$  with respect to  $y_{B_1}$ .

**Table 6**

A set of 6 modified positions for a planar four-bar linkage.

Positions	$x_P$ -Coordinate (mm)	$y_P$ -Coordinate (mm)	$x_Q$ -Coordinate (mm)	$y_Q$ -Coordinate (mm)
1	1.046800	1.382700	2.577900	1.777300
2	1.227700	1.752200	2.808300	1.795700
3	0.684600	1.987400	2.264400	1.921500
4	-0.080300	1.886300	1.500700	1.864300
5	-0.256500	1.325300	1.315600	1.494400
6	-0.316000	0.867500	1.189100	1.352100

**Table 7**

The approximate circle point and centre point corresponding to the positions in Table 6.

Circle point $B_1$ (mm)	Circle point $C_1$ (mm)	Center point $A$ (mm)	Center point $D$ (mm)
(0.846858, 0.0687262)	(2.983870, 1.645900)	(0.0941398, 0.0812037)	(2.574990, 0.510506)

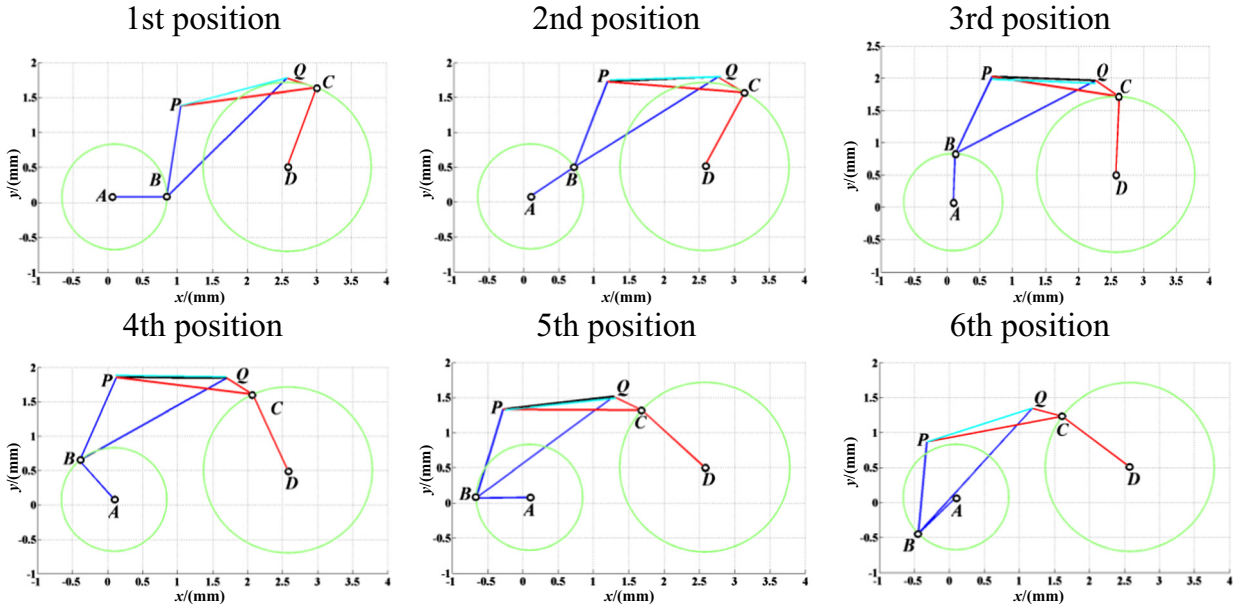


**Fig. 10.** A mechanism approximately meeting 6 different positions. (For interpretation of the references to color in this figure, the reader is referred to the web version of this article.)

Solving partial derivative equation set in Eq. (2.22) presents the stationary points. Assume that

$$\begin{cases} a = \frac{\partial^2 f(x_{B_1}, y_{B_1})}{\partial x_{B_1}^2} \\ b = \frac{\partial^2 f(x_{B_1}, y_{B_1})}{\partial x_{B_1} \partial y_{B_1}} \\ c = \frac{\partial^2 f(x_{B_1}, y_{B_1})}{\partial y_{B_1}^2} \end{cases} \quad (2.23)$$

According to calculus knowledge, the extreme values of  $f(x_{B_1}, y_{B_1})$  occur at  $a > 0$  and  $ac - b^2 > 0$ . The minimum value point can be found when these solutions are substituted into Eq. (2.21). Therefore, the circle point  $(x_{B_1}, y_{B_1})$  is obtained. It will be an accurate solution when the positions specified meet the requirements of the circle point; otherwise it is an approximate solution. Substituting the coordinates of the circle point into Eq. (2.16), the coefficients of the equation are all known. Rearranging equation set in Eq. (2.16) presents

$$\mathbf{K}\mathbf{x}_2 = \mathbf{h} \quad (2.24)$$

$$\text{where } \mathbf{K} = \begin{bmatrix} c_{21} & c_{22} \\ c_{31} & c_{32} \\ \vdots & \vdots \\ c_{n1} & c_{n2} \end{bmatrix}, \mathbf{x}_2 = \begin{bmatrix} x_A \\ y_A \end{bmatrix} \text{ and } \mathbf{h} = - \begin{bmatrix} c_{23} \\ c_{33} \\ \vdots \\ c_{n3} \end{bmatrix}.$$

**Table 8**

Errors between the accurate positions and the approximate positions.

Positions	$\varepsilon_P$ (mm)	$\varepsilon_Q$ (mm)
1	$1.490116 \times 10^{-8}$	$2.228243 \times 10^{-8}$
2	0.168095	0.163256
3	0.213522	0.201419
4	0.180981	0.177699
5	0.149669	0.159126
6	0.0810804	0.100795
Average	0.132225	0.133716

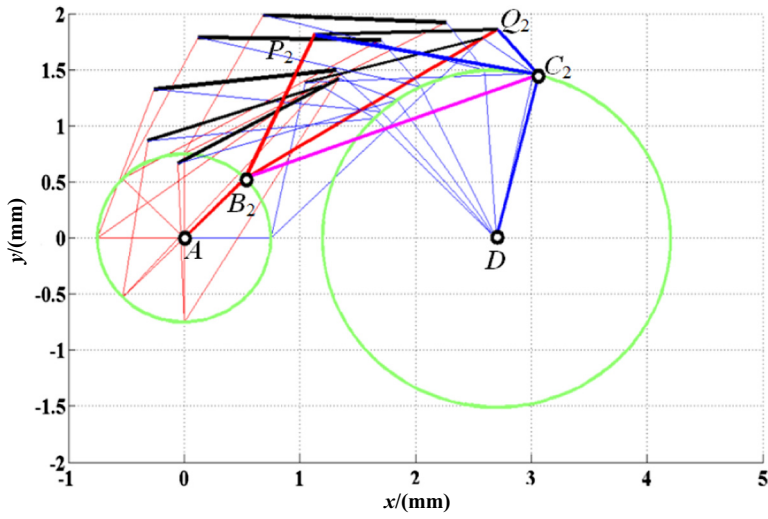


**Fig. 11.** Mechanism in the second position.

It is called overdetermined linear system when the number of equations is more than the number of unknown variables. For example,

$$\mathbf{Ax} = \mathbf{b}$$

where  $\mathbf{A} = \begin{bmatrix} a_{11} & a_{12} & \cdots & a_{1n} \\ a_{21} & a_{22} & \cdots & a_{2n} \\ \vdots & \vdots & \ddots & \vdots \\ a_{m1} & a_{m2} & \cdots & a_{mn} \end{bmatrix}$ ,  $\mathbf{b} = [b_1 \ b_2 \ \cdots \ b_m]^T$ ,  $\mathbf{x} \in R^n$ ,  $\mathbf{b} \in R^m$  and  $m > n$ .

To obtain the best approximate solutions, one needs to find the value of  $\mathbf{x}$  to satisfy the condition that

$$\min F(\mathbf{x}) = \sum_{i=1}^m \left( b_i - \sum_{j=1}^n a_{ij}x_j \right)^2 = \|\mathbf{b} - \mathbf{Ax}\|^2 \quad (2.25)$$

where  $\min F(\mathbf{x})$  indicates the minimum value of function  $F(\mathbf{x})$ .

For the function  $F(\mathbf{x})$ , the minimum value of it occurs when the partial derivatives are equal to 0, namely

$$\frac{\partial F}{\partial x_k} = -2 \sum_{i=1}^m a_{ik} \left( b_i - \sum_{j=1}^n a_{ij}x_j \right) = 0, \quad (k = 1, 2, \dots, n). \quad (2.26)$$

**Table 9**

Seven specified positions for the planar four-bar linkage.

Positions	$x_P$ -coordinate (mm)	$y_P$ -coordinate (mm)	$x_Q$ -coordinate (mm)	$y_Q$ -coordinate (mm)
1	1.046800	1.382700	2.577900	1.777300
2	1.127700	1.812200	2.708300	1.855700
3	0.684600	1.987400	2.264400	1.921500
4	0.119700	1.786300	1.700700	1.764300
5	-0.256500	1.325300	1.315600	1.494400
6	-0.316000	0.867500	1.189100	1.352100
7	-0.051700	0.663300	1.335700	1.421600

**Table 10**

Solutions for the circle point and centre point listed in Table 10.

Circle point $B_1$ (mm)	Circle point $C_1$ (mm)	Center point $A$ (mm)	Center point $D$ (mm)
(0.749685, -0.000162)	(3.017259, 1.466166)	(-0.000386, -0.000153)	(2.6996, -0.004914)

Expanding Eq. (2.26) and rearranging the variables presents

$$\left\{ \begin{array}{l} \sum_{i=1}^m a_{j1} \left( \sum_{j=1}^n a_{ij} x_j \right) = \sum_{i=1}^m a_{i1} b_i \\ \sum_{i=1}^m a_{i2} \left( \sum_{j=1}^n a_{ij} x_j \right) = \sum_{i=1}^m a_{i2} b_i \\ \vdots \\ \sum_{i=1}^m a_{in} \left( \sum_{j=1}^n a_{ij} x_j \right) = \sum_{i=1}^m a_{in} b_i. \end{array} \right. \quad (2.27)$$

Equation set in Eq. (2.27) can be further simplified as

$$\left\{ \begin{array}{l} \sum_{j=1}^n \mathbf{a}_1^T \mathbf{a}_j x_j = \mathbf{a}_1^T \mathbf{b} \\ \sum_{j=1}^n \mathbf{a}_2^T \mathbf{a}_j x_j = \mathbf{a}_2^T \mathbf{b} \\ \vdots \\ \sum_{j=1}^n \mathbf{a}_n^T \mathbf{a}_j x_j = \mathbf{a}_n^T \mathbf{b} \end{array} \right. \quad (2.28)$$

where  $\mathbf{a}_j^T$  denotes the transpose of  $\mathbf{a}_j$  and  $\mathbf{a}_j = [a_{1j} \ a_{2j} \ \dots \ a_{mj}]^T$  ( $j = 1, 2, \dots, n$ ).

Rearranging the equation again, one obtains

$$\mathbf{A}^T \mathbf{A} \mathbf{x} = \mathbf{A}^T \mathbf{b} \quad (2.29)$$

where  $\mathbf{A} = [\mathbf{a}_1 \ \mathbf{a}_2 \ \dots \ \mathbf{a}_n]$  and  $\mathbf{a}_j = [a_{1j} \ a_{2j} \ \dots \ a_{mj}]^T$  ( $j = 1, 2, \dots, n$ ).

Considering that  $m \geq n$ ,  $\mathbf{A}^T \mathbf{A}$  is an  $n \times n$  full rank square matrix, the general solution of  $\mathbf{x}$  in Eq. (2.29) can be expressed as:

$$\mathbf{x} = (\mathbf{A}^T \mathbf{A})^{-1} \mathbf{A}^T \mathbf{b} \quad (2.30)$$

where  $(\mathbf{A}^T \mathbf{A})^{-1} \mathbf{A}^T$  denotes the pseudo inverse of  $\mathbf{A}$  and  $(\mathbf{A}^T \mathbf{A})^{-1} \mathbf{A}^T = \mathbf{A}^{-1}$  when  $\mathbf{A}$  is an  $n \times n$  full rank matrix. This method is called the least square method.

**Table 11**

Seven modified positions for the planar four-bar linkage corresponding to those listed in Table 9.

Positions	$x_p$ -Coordinate (mm)	$y_p$ -Coordinate (mm)	$x_Q$ -Coordinate (mm)	$y_Q$ -Coordinate (mm)
1	1.046800	1.382700	2.577900	1.777300
2	1.227700	1.752200	2.808300	1.795700
3	0.684600	1.987400	2.264400	1.921500
4	-0.080300	1.886300	1.500700	1.864300
5	-0.256500	1.325300	1.315600	1.494400
6	-0.316000	0.867500	1.189100	1.352100
7	-0.001700	0.663300	1.385700	1.421600

**Table 12**

Approximate circle point and centre point corresponding to the positions in Table 11.

Circle point $B_1$ (mm)	Circle point $C_1$ (mm)	Center point $A$ (mm)	Center point $D$ (mm)
(0.819348, 0.055679)	(3.001470, 1.756439)	(0.064983, 0.073748)	(2.621502, 0.539307)

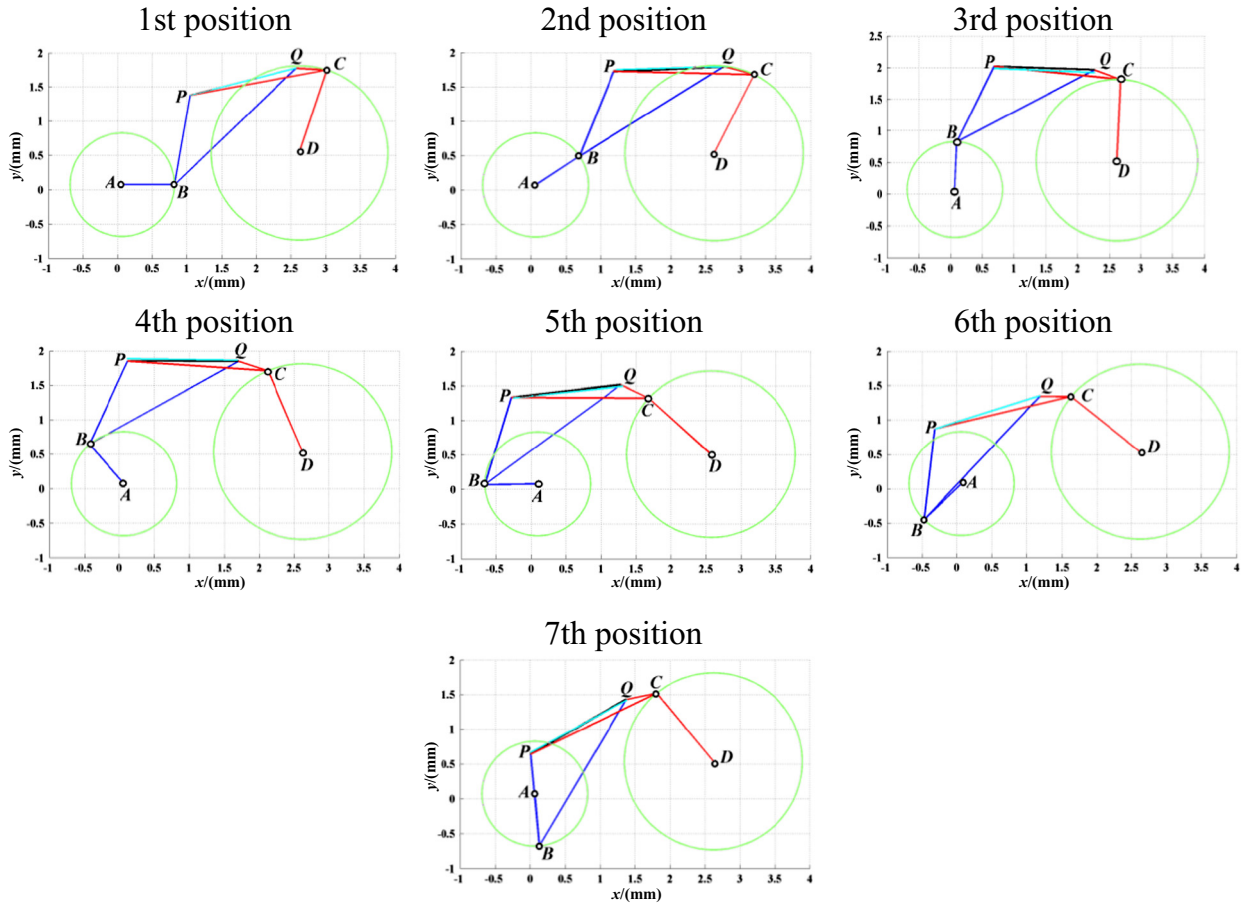


**Fig. 12.** A mechanism approximately meeting 7 different positions. (For interpretation of the references to color in this figure, the reader is referred to the web version of this article.)

Therefore, the general solution of  $\mathbf{x}_2$  in Eq. (2.24) can be obtained with Eq. (2.30):

$$\mathbf{x}_2 = (\mathbf{K}^T \mathbf{K})^{-1} \mathbf{K}^T \mathbf{h} \quad (2.31)$$

where  $(\mathbf{K}^T \mathbf{K})^{-1} \mathbf{K}^T = \mathbf{K}^{-1}$  when  $\mathbf{K}$  is a  $2 \times 2$  full rank matrix.

The results expressed by Eq. (2.31) will be the precise solution if the specified positions satisfy the circle point requirements; otherwise, the results will be the best approximate solutions for the prescribed multi-position requirements.

To satisfy the real applications, the Grashof conditions should also be discussed. As these problems have been investigated repeatedly and a lot of good means to select and optimize the planar four-bar motion generators with respect to Grashof conditions have been proposed [14,38,39], this paper no longer discusses these issues.

Because the augmented coefficient matrices,  $\mathbf{C}$ , for 2- and 3-position problems are  $1 \times 3$  and  $2 \times 3$ , respectively; Eq. (2.20) will therefore always hold. The solutions for the circle point  $B_1$  can be any point within the plane that the link locates, for 2- and 3-position problems. So in this section, examples will concentrate on the 4-, 5- and more-position designs.

**Table 13**

Errors between the accurate positions and the approximate positions.

Positions	$\varepsilon_P$ (mm)	$\varepsilon_Q$ (mm)
1	$1.490116 \times 10^{-8}$	$1.486653 \times 10^{-8}$
2	0.167374	0.162601
3	0.208832	0.193814
4	0.181070	0.175214
5	0.159767	0.172214
6	0.114452	0.139415
7	0.0757743	0.0937926
Average	0.129610	0.120465

**Table 14**

8 accurate positions for a planar four-bar linkage.

Positions	$x_P$ -Coordinate (mm)	$y_P$ -Coordinate (mm)	$x_Q$ -Coordinate (mm)	$y_Q$ -Coordinate (mm)
1	1.046800	1.382700	2.577900	1.777300
2	1.127700	1.812200	2.708300	1.855700
3	0.684600	1.987400	2.264400	1.921500
4	0.119700	1.786300	1.700700	1.764300
5	−0.256500	1.325300	1.315600	1.494400
6	−0.316000	0.867500	1.189100	1.352100
7	−0.051700	0.663300	1.335700	1.421600
8	0.469100	0.882600	1.851300	1.650300

**Table 15**

Solutions for the circle points and their center points corresponding to the position problem in Table 13.

Circle point $B_1$ (mm)	Circle point $C_1$ (mm)	Center point $A$ (mm)	Center point $D$ (mm)
(0.749755, −0.000061)	(3.017255, 1.466168)	(−0.000271, −0.000030)	(2.699542, −0.005128)

### 2.3. Design of planar four-bar linkages with 4 accurate positions

The coordinates of circle point and its center point satisfy equation set in Eq. (2.10) when 4 specified positions of the link are known. The augmented coefficient matrix of the constraint equation set is

$$\mathbf{C}_{3 \times 3} = \begin{bmatrix} C_{21} & C_{22} & C_{23} \\ C_{31} & C_{32} & C_{33} \\ C_{41} & C_{42} & C_{43} \end{bmatrix}. \quad (2.32)$$

According to Eq. (2.19), there is the following relationship because  $\mathbf{C}_{3 \times 3}$  is a square matrix:

$$|(\mathbf{M})_{3 \times 3}| = |\mathbf{C}_{3 \times 3}^T \mathbf{C}_{3 \times 3}| = |\mathbf{C}_{3 \times 3}^T| \cdot |\mathbf{C}_{3 \times 3}| = |\mathbf{C}_{3 \times 3}|^2 = 0$$

which can be simplified as

$$|\mathbf{C}_{3 \times 3}| = 0. \quad (2.33)$$

This again proves Eq. (2.12). Suppose that there are four different positions of the link which are listed in Table 1.

Substituting these parameters into Eq. (2.33), the precise circle point curve can be drawn. Fig. 8 shows the circle point loci that satisfy the four positions in Table 1.

Substituting the coordinates of a point from the circle point curve in Fig. 8 into any two equations of Eqs. (2.10) or (2.31), the exact center point coordinates can be obtained. For example, the center point can be expressed with Eq. (2.9) when the first two equations

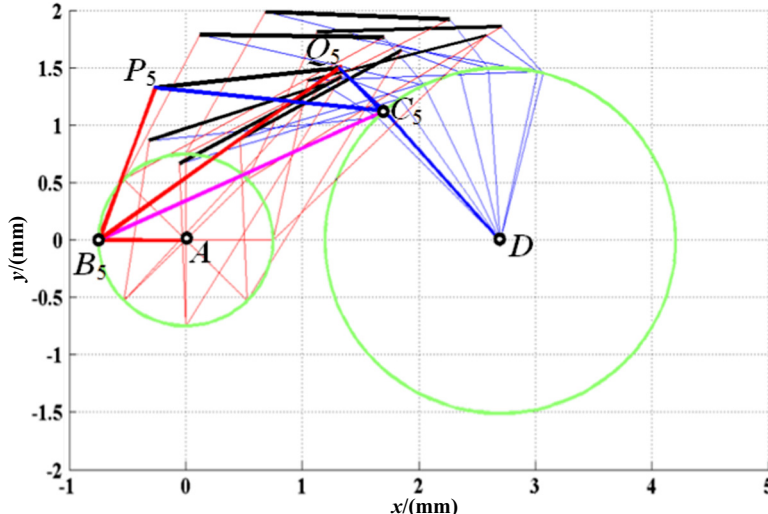


Fig. 13. Mechanism in the fifth position.

**Table 16**

8 modified positions of a planar four-bar linkage corresponding to those listed in Table 14.

Positions	$x_P$ -Coordinate (mm)	$y_P$ -Coordinate (mm)	$x_Q$ -Coordinate (mm)	$y_Q$ -Coordinate (mm)
1	1.046800	1.382700	2.577900	1.777300
2	1.227700	1.752200	2.808300	1.795700
3	0.684600	1.987400	2.264400	1.921500
4	−0.080300	1.886300	1.500700	1.864300
5	−0.256500	1.325300	1.315600	1.494400
6	−0.316000	0.867500	1.189100	1.352100
7	−0.001700	0.663300	1.385700	1.421600
8	0.489100	0.852600	2.808300	1.795700

**Table 17**

Approximate circle point and centre point corresponding to the positions in Table 16.

Circle point $B_1$ (mm)	Circle point $C_1$ (mm)	Center point $A$ (mm)	Center point $D$ (mm)
(0.852813, 0.092069)	(3.032621, 1.789466)	(0.102542, 0.108504)	(2.683970, 0.458268)

of equation set in Eq. (2.10) are selected. As previous literature investigated this problem repeatedly, this paper does not discuss it again.

#### 2.4. Design of planar four-bar linkages with 5 positions

When 5 positions for the link are specified, the circle points can be solved with the process discussed in Section 2.2. The results obtained here will be accurate if the 5-position problem has exact solutions; otherwise, the results will be the best approximate solutions for the 5-position problem. Table 2 lists the 5 positions a planar four-bar linkage should trace.

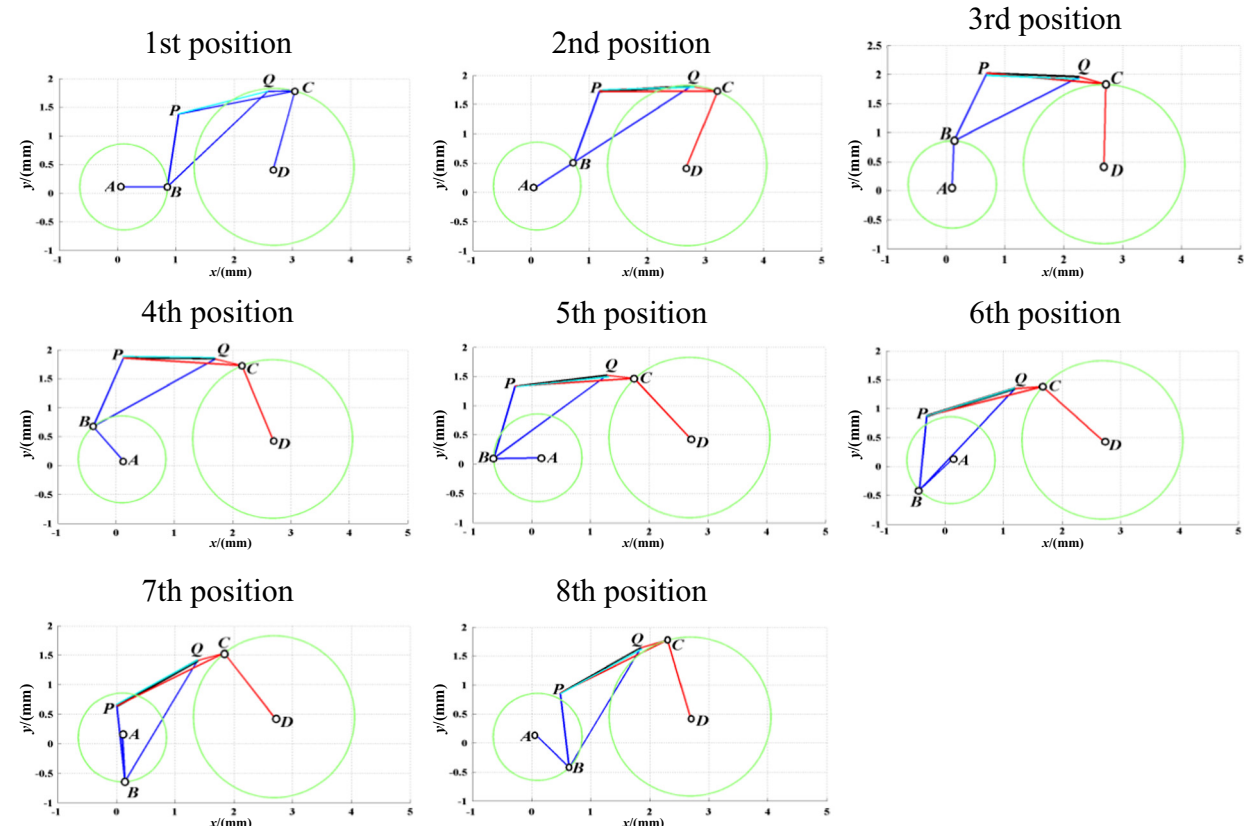


**Fig. 14.** A mechanism approximately satisfying 8 different positions. (For interpretation of the references to color in this figure, the reader is referred to the web version of this article.)

**Table 18**

Errors between the accurate positions and approximate positions of the 8 positions listed in Table 14 and Table 16.

Positions	$\varepsilon_B$ (mm)	$\varepsilon_Q$ (mm)
1	$1.490116 \times 10^{-8}$	0
2	0.212232	0.219992
3	0.211273	0.197230
4	0.174490	0.174950
5	0.168812	0.188693
6	0.111195	0.126478
7	0.110296	0.104494
8	0.0488729	0.0634161
Average	0.130084	0.134407

Substituting the parameters of Table 2 into Eq. (2.19) yields

$$\mathbf{M} = \begin{bmatrix} (0.702454x_{B_1}^2 - 3.595620x_{B_1}y_{B_1} + 96.533200x_{B_1} \\ + 4.898390y_{B_1}^2 - 258.246000y_{B_1} + 3490.950000) & (1.797810x_{B_1}^2 - 4.195930x_{B_1}y_{B_1} + 105.939000x_{B_1} \\ - 1.797810y_{B_1}^2 - 4.195930x_{B_1}y_{B_1} + 105.939000x_{B_1} \\ - 1.797810y_{B_1}^2 + 97.966700y_{B_1} - 1054.190000) & (-53.262400x_{B_1}^2 + 116.772000x_{B_1}y_{B_1} - 2776.090000x_{B_1} \\ + 51.828800y_{B_1}^2 - 3684.600000y_{B_1} + 53181.100000) \\ (1.797810x_{B_1}^2 + 3.595620x_{B_1}y_{B_1} - 99.400300x_{B_1} \\ - 1.797810y_{B_1}^2 + 46.368000y_{B_1} + 3034.540000) & (-134.539000x_{B_1}^2 - 105.091000x_{B_1}y_{B_1} + 4331.140000x_{B_1} \\ - 17.767500y_{B_1}^2 - 664.276000y_{B_1} - 29219.300000) \\ (-53.262400x_{B_1}^2 + 116.772000x_{B_1}y_{B_1} - 2776.090000x_{B_1} \\ + 51.828800y_{B_1}^2 - 3684.600000y_{B_1} + 53181.100000) & (4236.810000x_{B_1}^2 + 1731.640000x_{B_1}y_{B_1} - 122679.000000x_{B_1} \\ + 2288.690000y_{B_1}^2 - 33612.800000y_{B_1} + 921452.000000) \end{bmatrix}. \quad (2.34)$$

Substituting Eq. (2.34) into Eq. (2.20) presents

$$\begin{aligned} |\mathbf{M}| = & 39.178500x_{B_1}^6 - 185.130000x_{B_1}^5y_{B_1} + 4608.050000x_{B_1}^5 \\ & - 370.259000x_{B_1}^3y_{B_1}^3 + 1955.700000x_{B_1}^3y_{B_1}^2 + 902479.000000x_{B_1}^3y_{B_1} - 1.941440 \times 10^7x_{B_1}^3 \\ & - 83039.400000x_{B_1}^2y_{B_1}^3 + 3460755.000000x_{B_1}^2y_{B_1}^2 - 6.402050 \times 10^7x_{B_1}^2y_{B_1} + 4.939500 \times 10^8x_{B_1}^2y_{B_1}^5 \\ & - 2652.350000x_{B_1}y_{B_1}^4 + 2919555.000000x_{B_1}y_{B_1}^3 - 1.744070 \times 10^8x_{B_1}y_{B_1}^2 + 3.297460 \times 10^9x_{B_1}y_{B_1} - 1.485650 \times 10^{10}x_{B_1} \\ & + 355.610000y_{B_1}^6 - 69114.300000y_{B_1}^5 + 5022288.000000y_{B_1}^4 - 1.765640 \times 10^8y_{B_1}^3 + 3.572560 \times 10^9y_{B_1}^2 - 5.127750 \times 10^{10}y_{B_1} \\ & + 4.507380 \times 10^{11} \\ = & 0. \end{aligned} \quad (2.35)$$

There are four different real solutions for the circle point  $B_1(x_{B_1}, y_{B_1})$  for Eq. (2.35) which are shown in Table 3. Substituting these solutions into Eq. (2.30) allows one to obtain the coordinates of the center point. For example, substituting the first solution of point  $B_1$  into Eq. (2.30) presents

$$\begin{bmatrix} 1.028114 & 3.686569 \\ -6.356135 & -28.006752 \\ -11.429996 & -73.117632 \\ -8.202628 & -39.230632 \end{bmatrix} \begin{bmatrix} x_A \\ y_A \end{bmatrix} = \begin{bmatrix} -42.181186 \\ 598.922840 \\ 2552.366548 \\ 973.119227 \end{bmatrix}. \quad (2.36)$$

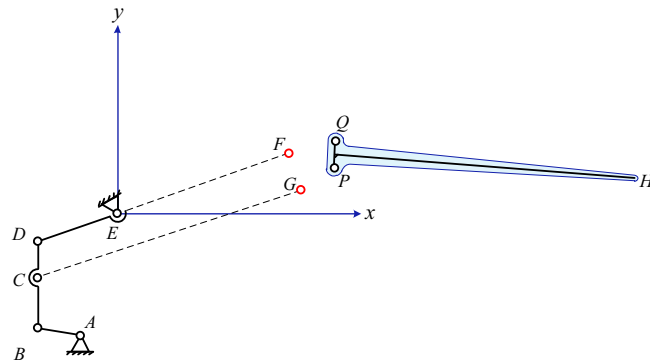
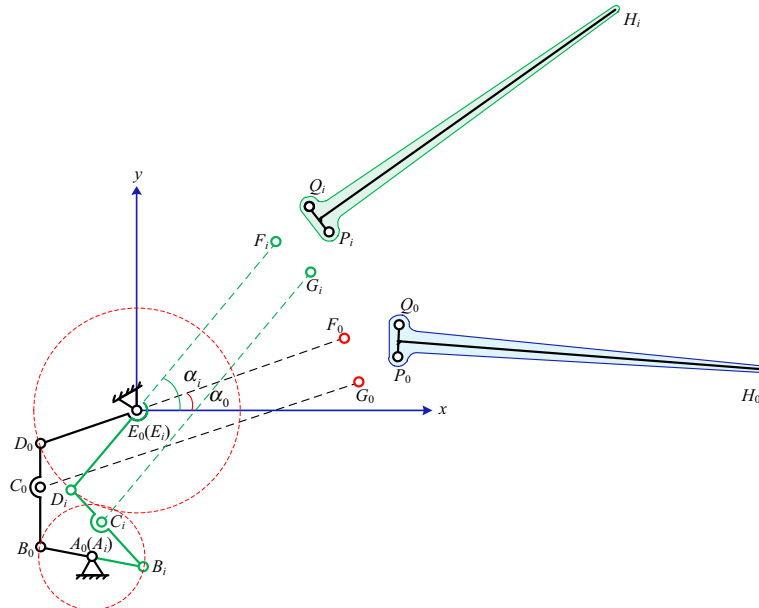


Fig. 15. Basic part with a coordinate system.



**Fig. 16.** Initial position and the  $i$ th position. (For interpretation of the references to color in this figure legend, the reader is referred to the web version of this article.)

Solving Eq. (2.36) with the formula in Eq. (2.31) yields

$$\begin{cases} x_A = 191.467702 \\ y_A = -64.838556 \end{cases}$$

Similarly, the other center points corresponding to the circle points can be gained. The 4 different solutions for the specified 5-position problem are listed in Table 3.

According to Burmester's theory, planar revolute jointed four-bar linkage could exactly trace 5 arbitrary positions with the prescribed poses at most. But the method proposed in this paper could also present a best approximate result when the 5-position design has no precise solution. The same is true for more prescribed positions which will be discussed next.

## 2.5. Design of planar four-bar linkages with more approximate positions

Table 4 lists 6 positions for a planar four-bar linkage. The solutions for the circle point  $B_1$  and its center point  $A$ , the circle point  $C_1$  and its center point  $D$  can be obtained with the process discussed in Section 2.2.

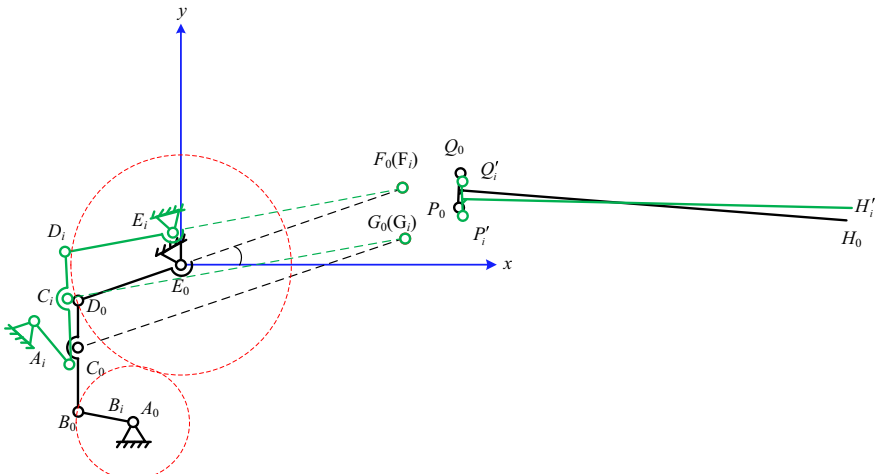


**Fig. 17.**  $i$ th position after the rotation and translation.

**Table 19**

Eight series of positions generated from the flapping wing.

Positions	$x_P$ -Coordinate (mm)	$y_P$ -Coordinate (mm)	$x_Q$ -Coordinate (mm)	$y_Q$ -Coordinate (mm)
1	198.1325	163.8906	192.3043	175.3371
2	184.7892	173.8754	181.0724	186.1708
3	240.2945	76.7505	243.6244	89.1563
4	176.8725	177.9135	175.5048	190.6853
5	221.1555	116.0251	224.8183	128.3366
6	175.6542	176.2457	176.4870	189.0636
7	201.0169	145.7083	204.5192	158.0665
8	183.3543	166.8456	184.8885	180.5874

Generally, there are only approximate solutions for circle points and center points when more than 5 positions for the link are specified. Fortunately, the 6-position design prescribed in Table 4 has accurate solutions which could be directly gained with Eq. (2.20) or (2.21)–(2.24), (2.31). The solutions for the center point and circle points are listed in Table 5 which demonstrates the effectiveness of the method proposed in this paper. The mechanism exactly satisfying the 6 positions prescribed in Table 4 is illustrated by Fig. 9. The quadrangle  $B_1C_1Q_1P_1$  shown in Fig. 9 represents link  $B_1C_1$ .

There are only approximate solutions when these 6 positions are changed a little. Suppose the changed 6 positions are listed in Table 6 where only the second and fourth positions are altered near their original places.

The approximate circle point and center point corresponding to the positions in Table 6 are represented in Table 7, and the mechanism approximately satisfying the positions prescribed in Table 6 is illustrated in Fig. 10. The light blue bold lines represent the accurate positions specified by Table 6 and the dark bold lines are the real positions that the planar four-bar mechanism could approximately trace.

Then, the errors between the accurate positions and the approximate positions are calculated. Table 8 represents the results. The absolute errors of positions are measured by the following equations:

$$\begin{cases} \varepsilon_P = \sqrt{(x_{P_i} - x_{P'_i})^2 + (y_{P_i} - y_{P'_i})^2} \\ \varepsilon_Q = \sqrt{(x_{Q_i} - x_{Q'_i})^2 + (y_{Q_i} - y_{Q'_i})^2} \end{cases} \quad (2.37)$$

where  $\varepsilon_P$  and  $\varepsilon_Q$  represent the errors at points  $P$  and  $Q$ , respectively, and  $(x_{P_i}, y_{P_i})$  represent the coordinates of the  $i$ th accurate position and  $(x_{P'_i}, y_{P'_i})$  represent the coordinates of the  $i$ th approximate position for calculation. From Table 8, one knows that the maximum error occurs at the 3rd position, the error of point  $P$  is equal to 0.213522 mm and the error of point  $Q$  is 0.201419 mm.

When 7 positions are specified, the solutions for the circle point  $B_1$  and its center point  $A$ , the circle point  $C$  and its center point  $D$  can be obtained with the similar process. Fig. 11 illustrates the planar four-bar linkage that exactly meets the 7 positions prescribed in Table 9. Fig. 11 presents the case when the mechanism is in the second position for the specified 7 positions. The solutions for the circle point and center point are listed in Table 10.

There are only approximate solutions when these 7 arbitrary positions are specified. Suppose that the 7 positions are listed in Table 11 where the second, fourth and seventh positions are different compared with those listed in Table 9.

The approximate circle point and center point corresponding to the positions in Table 11 are represented in Table 12, and the mechanism approximately satisfying the positions prescribed in Table 11 is shown in Fig. 12. The light blue bold lines represent the accurate positions specified by Table 11 and the dark bold lines are the real positions that the planar mechanism could approximately trace.

The errors between the accurate positions and the approximate positions are shown in Table 13. From Table 13, one knows that the maximum error occurs at the 3rd position, the error of point  $P$  is equal to 0.28832 mm and the error of point  $Q$  is equal to 0.19381 mm.

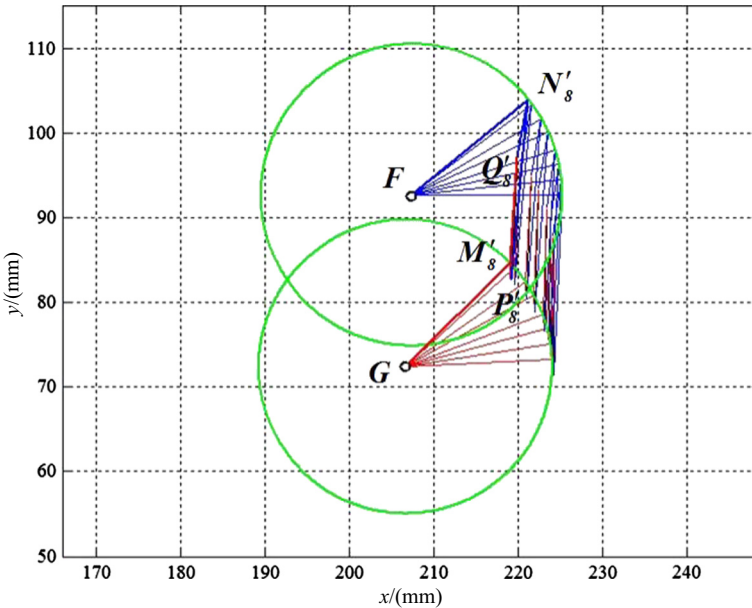
When 8 accurate positions are prescribed in Table 14 the solutions for the circle point  $B_1$  and its center point  $A$ , the circle point  $C_1$  and its center point  $D$  can be obtained with the same process which are listed in Table 15.

Fig. 13 shows the case when the mechanism moves to the fifth position for the specified 8-position problem.

**Table 20**

Eight series of positions after coordinate transformation for those listed in Table 19.

Positions	$x_P$ -Coordinate (mm)	$y_P$ -Coordinate (mm)	$x_Q$ -Coordinate (mm)	$y_Q$ -Coordinate (mm)
1	224.1926	76.7505	224.2586	85.9116
2	223.9907	79.5905	224.1240	87.7434
3	223.5946	81.2414	223.8019	89.5445
4	223.0411	81.6519	223.3270	91.2108
5	222.0071	80.6142	222.4196	93.3963
6	221.0177	78.3141	221.5466	94.9539
7	219.6197	75.0296	220.3214	96.6669
8	219.0822	71.1750	219.8557	97.2189



**Fig. 18.** Mechanism in the eighth position.

There are also only approximate solutions when these 8 arbitrary positions are specified. Table 16 shows the 8 positions of a planar four-bar linkage where the second, fourth, seventh and eighth positions are different from those listed in Table 14.

The approximate circle point and center point corresponding to the positions in Table 16 are represented in Table 17, and the mechanism approximately satisfying the positions prescribed in Table 16 is shown in Fig. 14. The light blue bold lines represent the accurate positions specified by Table 14 and the dark bold lines are the real positions that the planar mechanism could approximately trace.

The errors between the accurate positions and the approximate positions are listed in Table 18. From Table 18, one knows that the maximum error occurs at the 2nd position, the error of point  $P$  is equal to 0.212232 mm and the error of point  $Q$  is equal to 0.219992 mm.

The method can also be directly used when more positions are required. The examples illustrate that the unified formula is very convenient in engineering applications for the design of planar four-bar linkages with  $n$  specified positions. It can search the accurate results when there are such solutions for the specified  $n$  precise positions; otherwise, the best approximate solutions will be found. The merits of the method proposed in this paper is that the engineers could directly obtain the planar four-bar linkages when the specified positions are known without the need to check whether all center/circle-point curves have common cross point.

### 3. Design of planar four-bar linkage for a flapping wing robot

Hereto the design of a flapping wing robot can be discussed. A coordinate system is established by setting the origin at the fixed joint  $E$ ,  $x$ -axis is rightward along the horizontal direction and  $y$ -axis is the vertical axis as shown in Fig. 15. According to the 8-position requirement of the wing of a real seagull, a crank-rocker linkage  $ABDE$  shown in Fig. 15 is designed. That is to say, the coordinates of points  $A$ ,  $B$ ,  $C$ ,  $D$ , and  $E$  can be obtained in line with the above process. According to the eight crucial positions shown in Fig. 2, the eight sets of data, angle  $\alpha$  and point  $P$ ,  $Q$  and  $H$  are obtained, where  $\alpha$  is the angle between the inner wing and horizontal direction. What needs to be confirmed are the coordinates of points  $F$  and  $G$ , which will be solved with the method proposed in this paper.

Now the condition of the mechanism when it comes to the  $i$ th position during the upstroke is illustrated in Fig. 16. The  $i$ th position is shown in green line while the black line is the initial position of the mechanism (1st position). Consider the whole mechanism of the  $i$ th position as a rigid body, then rotate and translate the whole part until point  $F_0$  and  $F_i$  are coincident and points  $G_0$  and  $G_i$  are coincident. The consequence is shown in Fig. 17.

After the rotation and translation, it generates a new group of the coordinates of points  $P_i$  and  $Q_i$ , which are marked as  $P'_i$ ,  $Q'_i$ . There are eight crucial positions during the upstroke, so seven series of points  $P'_i$ ,  $Q'_i$  ( $i = 1, 2, 4, 5, 6, 7$ ) could be obtained. It is eight series in

**Table 21**

Coordinates of the circle points and centre points of the four-bar mechanism shown in Fig. 18.

Circle point $M'_1$ (mm)	Circle point $N'_1$ (mm)	Center point $F$ (mm)	Center point $G$ (mm)
(224.0114, 73.3305)	(225.2203, 92.7107)	(207.3927, 92.6218)	(206.6669, 72.4312)

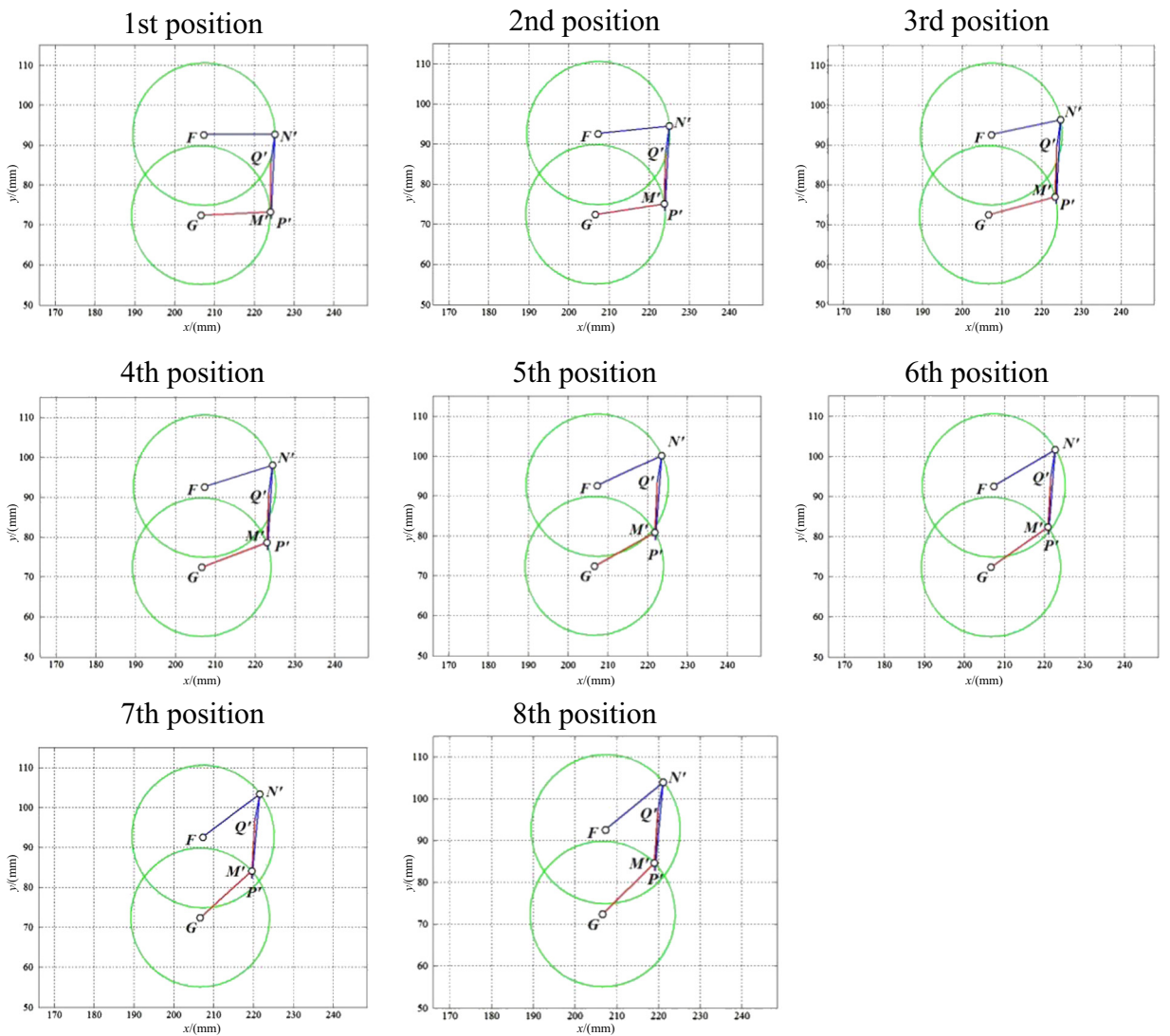


**Fig. 19.** A mechanism approximately satisfying 8 different positions.

total plusing points  $P_0$  and  $Q_0$ . The point  $F$  and point  $G$  can be obtained to approximately satisfy the eight positions by using the method that is proposed in Section 3. According to the process, it obtains eight series of positions  $P, Q$  as listed in Table 19. Table 20 shows the eight series of positions after the rotation and translation.

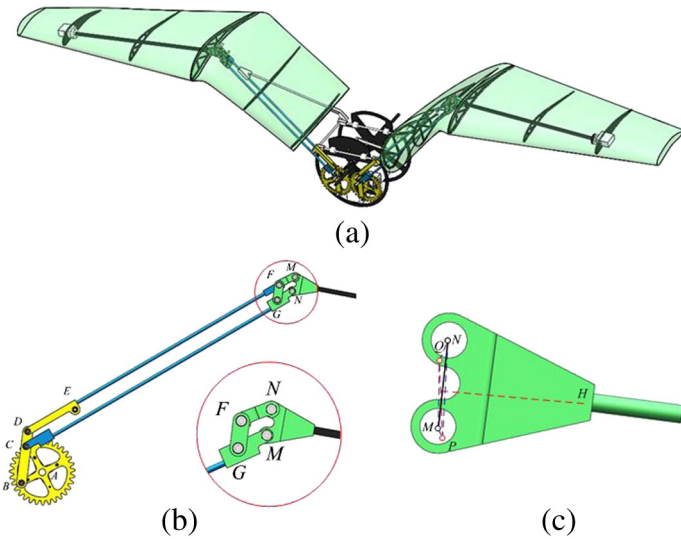
Fig. 18 shows the case when the mechanism passes through the specified 8 positions, respectively.

Table 21 shows the coordinates of the circle points and center points of the four-bar mechanism  $FGPQ$  shown in Fig. 18. The coordinate and orientation errors in every position are illustrated by Fig. 19. The errors between the accurate positions and the

**Table 22**

Errors between the accurate positions specified and the approximate positions.

Positions	$\varepsilon_P$ (mm)	$\varepsilon_Q$ (mm)
1	$1.192093 \times 10^{-7}$	0
2	0.315936	0.311827
3	0.44628	0.440097
4	0.540497	0.532536
5	0.644939	0.634622
6	0.71117	0.698991
7	0.778564	0.764361
8	0.799396	0.784462
Average	0.529594	0.520862



**Fig. 20.** Initial model of the robotic bird.

approximate positions are shown in [Table 22](#). From [Table 22](#), one knows that the maximum error occurs at the 8th position, the error of point  $P$  is equal to 0.799396 mm and the error of point  $Q$  is equal to 0.784462 mm.

With these parameters listed in [Table 22](#), the initial model of the robotic bird shown in [Fig. 20\(a\)](#) is designed. The main structure to achieve the flapping wing is composed of three basic four-bar linkages shown in [Fig. 20\(b\)](#). The rigid body that contains link  $MN$  and link  $PQ$  is shown in [Fig. 20\(c\)](#). The corresponding 8 positions of the robotic bird are shown in [Fig. 21](#). [Fig. 22](#) presents the prototype with the theoretical results which simulate the flapping process of the bird.

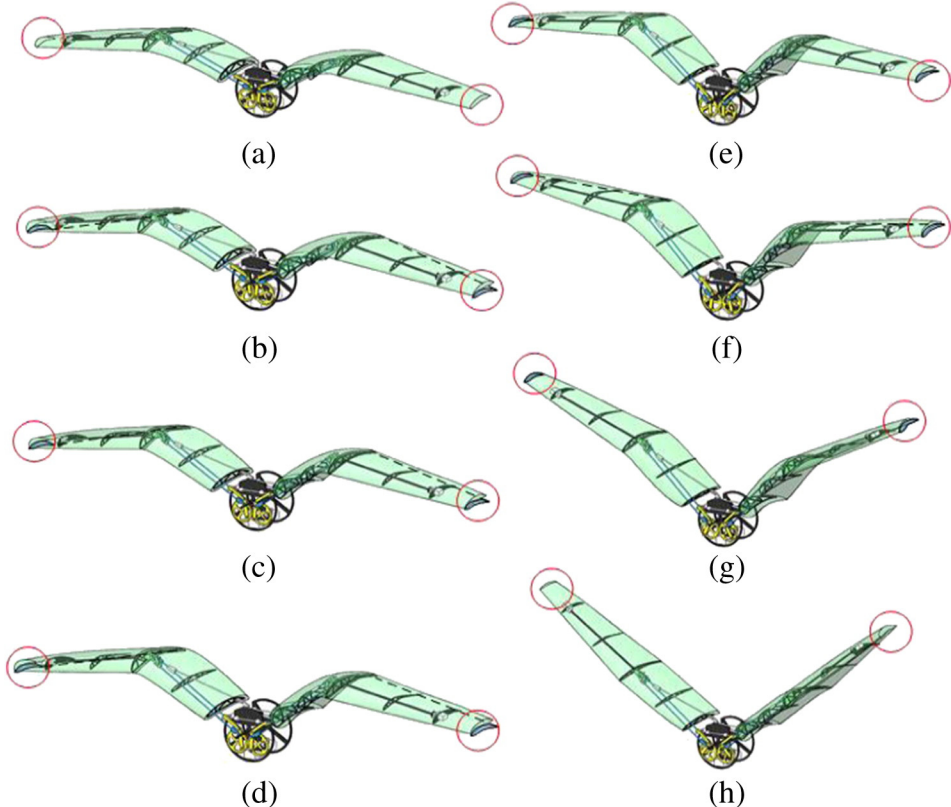


**Fig. 21.** Corresponding 8 positions of the robotic bird. (For interpretation of the references to color in this figure, the reader is referred to the web version of this article.)



**Fig. 22.** Real initial model of the robotic bird.

The flapping motion is generated through the three basic planar four-bar linkages while the twisting movement is realized through a generalized flexible joint distributed on the wing skin as shown in Fig. 23. The generalized flexible joint is controlled by a motor at the end of wing skin. Fig. 23(b) and (c) illustrates the motion of motor to imitate the twist of the wing. During the upstroke of flight, the generalized flexible joint is twisted down by the motor while it is twisted up during the downstroke of flight. One can also find the change of twisting of the generalized flexible joint in Fig. 21 shown in the red circles. In the beginning of the upstroke, the twisting angle is the maximum and it is decreasing with the upstroke of flight. It equals 0 when it approaches the end of upstroke. When downstroke starts, the generalized flexible joint is twisted in the opposite direction of the upstroke and the twisting angle is also the maximum one. It is decreasing with the downstroke of flight. It equals 0 when it comes to the end of downstroke. In the next cycle of flight, this process is repeated. The relationship between phases of flapping and twisting is retained by a controller.

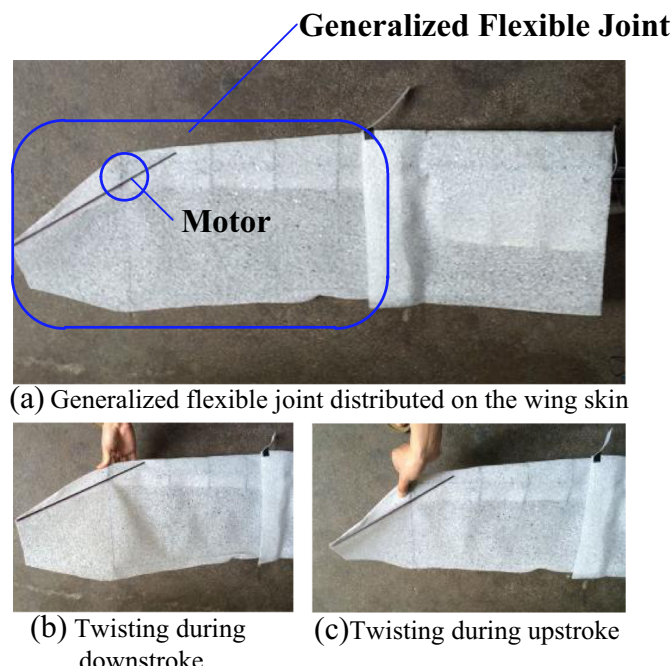


**Fig. 23.** Generalized flexible joint distributed on the wing skin.

## 4. Conclusions

This paper focuses on the design of a flapping wing robot and proposes a unified design formula for planar four-bar linkages with arbitrary  $n$  prescribed positions. The coordinates of the circle point at the first position were used as the design variables to build the distance constraint equations for the following successive positions through matrix transformation. Expanding the quadratic equations and eliminating the quadratic items of the coordinates of the center point, a set of linear equations were obtained. The augmented coefficient matrix consisting of the coordinates of circle point at the first position was then utilized to form a  $3 \times 3$ -matrix  $\mathbf{M}$ . Solutions of the circle points could be represented as  $|\mathbf{M}| = 0$  which provides a unified expression for the design of planar four-bar linkages. The least square method was used to get the best approximate solutions for the problem of more than 4 positions which might not have any exact solutions.

## Acknowledgment

This research was supported by the National Natural Science Foundation of China under Grant 50805083. The authors are grateful to Mr. Di Ai, Mr. Yunfei Liu and Mr. Jiajing Lin for their hard work and kind help in the design, manufacturing and assembly, and test of the flying robot.

## Appendix A

### Notation

$a$	Second partial derivative $\frac{\partial^2 f(x_{B_1}, y_{B_1})}{\partial x_{B_1}^2}$ .
$b$	Second partial derivative $\frac{\partial^2 f(x_{B_1}, y_{B_1})}{\partial x_{B_1} \partial y_{B_1}}$ .
$c$	Second partial derivative $\frac{\partial^2 f(x_{B_1}, y_{B_1})}{\partial y_{B_1}^2}$ .
$f(x_{B_1}, y_{B_1})$	Determinant function of matrix $\mathbf{M}$ .
$\frac{\partial f(x_{B_1}, y_{B_1})}{\partial x_{B_1}}$	Partial derivative of $f(x_{B_1}, y_{B_1})$ with respect to $x_{B_1}$ .
$g(\cdot)$	Lagrange function.
$\mathbf{h}$	$-[c_{23} c_{33} \dots c_{n3}]^T$ .
$\binom{m}{n}$	Number of the combination of $n$ from $m$ .
$n$	Number of positions.
$\mathbf{r}_{B_i}$	Absolute vector of joint $B_i$ .
$\mathbf{r}_{P_i}(i=1, 2, \dots)$	Absolute vector of joint $P_i$ .
$\mathbf{r}_{P_1 P_i}$	Absolute vector of $P_1 P_i$ .
$\mathbf{x}_3$	A 3-dimensional nonzero vector.
$\mathbf{x}_2$	A 2-dimensional nonzero vector.
$A$	Left center point.
$\mathbf{A}$	A Matrix
$B_i(i=1, 2, \dots)$	$i$ th left circle point of the link.
$C_i(i=1, 2, \dots)$	$i$ th right circle point of the link.
$\mathbf{C}_{3 \times 3}$	Coefficient matrix.
$D$	Right center point.
$\mathbf{K}$	$\begin{bmatrix} c_{21} & c_{31} & \dots & c_{n1} \\ c_{22} & c_{32} & \dots & c_{n2} \end{bmatrix}^T$ .
$\mathbf{M}$	Matrix composed of position parameters, $\mathbf{M} = \mathbf{C}_{(n-1) \times 3}^T \mathbf{C}_{(n-1) \times 3}$ .
$P_i Q_i(i=1, 2, \dots)$	$i$ th position of the link.
$R(\cdot)$	Rank of matrix “ $\cdot$ ”.
$\mathbf{R}(\theta_{1i})$	Transformation matrix from the $i$ th position to the first one.
$\theta_i(i=1, 2, \dots)$	$i$ th pose angle of the link.
$\theta_{1i}(i=1, 2, \dots)$	Relative pose angle of the $i$ th position with respect to the first one.
$ \cdot $	Determinant of matrix “ $\cdot$ ”.
$\ \cdot\ $	2-norm of vector “ $\cdot$ ”.

## References

- [1] A. Bergou, S. Xu, Z. Wang, Passive wing pitch reversal in insect flight, *J. Fluid Mech.* 591 (2007) 321–337.
- [2] T.L. Hedrick, T.L. Daniel, Flight control in the hawkmoth *Manduca sexta*: the inverse problem of hovering, *J. Exp. Biol.* 209 (2006) 3114–3130.

- [3] T.G. Chondros, The development of machine design as a science from classical times to modern era, *Int. Symp. Hist. Mach. Mech.* (2009) 62.
- [4] F.T. Muijres, L.C. Johansson, R. Barfield, M. Wolf, G.R. Spedding, A. Hedenstrom, Leading-edge vortex improves lift in slow-flying bats, *Science* 319 (2008) 1250–1253.
- [5] V. Arabagi, L. Hines, M. Sitti, Design and manufacturing of a controllable miniature flapping wing robotic platform, *Int. J. Robot. Res.* 31 (6) (2012) 785–800.
- [6] R.S. Hartenberg, J. Denavit, *Kinematic Synthesis of Linkages*, McGraw-Hill, New York, 1964.
- [7] T.G. Chondros, Archimedes life works and machines, *Mech. Mach. Theory* 45 (2010) 1766–1775.
- [8] K.H. Hunt, *Kinematic Geometry of Mechanisms*, Oxford University Press, New York, 1978.
- [9] C.H. Suh, C.W. Radcliffe, *Kinematics and Mechanisms Design*, Wiley, New York, 1978.
- [10] O. Bottema, B. Roth, *Theoretical Kinematics*, North-Holland, New York, 1979.
- [11] J. Angeles, *Spatial Kinematic Chains: Analysis, Synthesis, and Optimization*, Springer-Verlag, Berlin, 1982.
- [12] J.M. McCarthy, G.S. Soh, *Geometric Design of Linkages*, Springer, New York, 2011.
- [13] R.S. Hartenberg, J. Denavit, *Kinematic Synthesis of Linkages*, McGraw-Hill, New York, 1964.
- [14] Q. Shen, Y.M. Al-Smadi, P.J. Martin, K. Russell, R.S. Sodhi, An extension of mechanism design optimization for motion generation, *Mech. Mach. Theory* 44 (9) (2009) 1759–1767.
- [15] J.M. Prentis, The pole triangle, Burmester's theory and order and branching problems—I. The order problem, *Mech. Mach. Theory* 26 (1) (1991) 19–30.
- [16] L. Burmester, *Lehrbuch der Kinematik*, Arthur Felix Verlag, Leipzig, Germany, 1888.
- [17] K.J. Waldron, Location of Burmester synthesis solutions with fully rotatable cranks, *Mech. Mach. Theory* 13 (2) (1978) 125–137.
- [18] K.J. Waldron, R.T. Strong, Improved solutions of the branch and order problems of Burmester linkage synthesis, *Mech. Mach. Theory* 13 (2) (1978) 199–207.
- [19] A.C. Rao, Synthesis of 4-bar function-generators using geometric programming, *Mech. Mach. Theory* 14 (2) (1979) 141–149.
- [20] A. Ahmad, K.J. Waldron, Synthesis of adjustable planar 4-bar mechanisms, *Mech. Mach. Theory* 14 (6) (1979) 405–411.
- [21] A.G. Erdman, Three and four precision point kinematic synthesis of planar linkages, *Mech. Mach. Theory* 16 (3) (1981) 227–245.
- [22] C.H. Suh, C.W. Radcliffe, *Kinematics and Mechanism Design*, John Wiley and Sons, New York, 1978.
- [23] G.N. Sandor, A.G. Erdman, *Advanced Mechanism Design: Analysis and Synthesis*, vol. 2, Prentice-Hall, Englewood Cliffs, NJ, 1984.
- [24] K.H. Hunt, *Kinematic Geometry of Mechanisms*, Oxford University Press, London, 1978.
- [25] T. Koetsier, The centenary of Ludwig Burmester's "Lehrbuch der Kinematik", *Mech. Mach. Theory* 24 (1) (1989) 37–38.
- [26] A.D. Machine Dimarogonas, A. Design, CAD Approach, John Wiley and Sons, Inc., New York, 2001.
- [27] H. Nolle, Linkage coupler curve synthesis: a historical review—I. Developments up to 1875, *Mech. Mach. Theory* 9 (2) (1974) 147–168.
- [28] H. Nolle, Linkage coupler curve synthesis: a historical review—II. Developments after 1875, *Mech. Mach. Theory* 9 (3–4) (1974) 325–348.
- [29] H. Nolle, Linkage coupler curve synthesis: historical review—III. Spatial synthesis and optimization, *Mech. Mach. Theory* 10 (1) (1975) 41–55.
- [30] Y. Chen, J. Fu, A computational approach for determining location of Burmester solutions with fully rotatable cranks, *Mech. Mach. Theory* 34 (4) (1999) 549–558.
- [31] C. Chen, J. Angeles, A novel family of linkages for advanced motion synthesis, *Mech. Mach. Theory* 43 (7) (2008) 882–890.
- [32] T.H. Davies, J.E. Baker, A.G.R. Thompson, A finite 3-dimensional atlas of 4-bar linkages, *Mech. Mach. Theory* 14 (6) (1979) 389–403.
- [33] C.S. Lin, A.G. Erdman, Dimensional synthesis of planar triads: motion generation with prescribed timing for six precision positions, *Mech. Mach. Theory* 22 (5) (1987) 411–419.
- [34] T. Yang, J. Han, L. Yin, A unified synthesis method based on solution regions for four finitely separated and mixed "point-order" positions, *Mech. Mach. Theory* 46 (11) (2011) 1719–1731.
- [35] K.Y. Kim, B.M. Kwak, A modified selective precision synthesis technique for planar four-bar rigid-body guidance, *Proc. Inst. Mech. Eng. C J. Mech. Eng. Sci.* 209 (1) (1995) 39–47.
- [36] J.S. Chen, C.H. Chiang, Coordinations of coupler-line positions with input-link rotations by a planar four-bar linkage, *Mech. Mach. Theory* 27 (5) (1992) 555–561.
- [37] C. Sultan, S. Seeraram, R.K. Mehra, Deep space formation flying spacecraft path planning, *Int. J. Robot. Res.* 26 (4) (2007) 405–430.
- [38] C.R. Barker, A complete classification of planar four-bar linkages, *Mech. Mach. Theory* 20 (6) (1985) 535–554.
- [39] P.J. Martin, K. Russell, R.S. Sodhi, On mechanism design optimization for motion generation, *Mech. Mach. Theory* 42 (10) (2001) 1251–1263.